Ferdowsi University of Mashhad

Journal of Applied and Computational Sciences in Mechanics

Page Journal: mechanic-ferdowsi.um.ac.ir

Society of Manufacturing Engineering of Iran

Fault Diagnosis of a Reciprocating Compressor Valve Based on Neural

Hadi Kalani[1], Mohammad Afkanpour[2], Abutaleb Gholizadeh[3], Ahmad Hajipour[4]

10.22067/jacsm.2026.96210.1376

Reciprocating compressors are commonly used machinery for industrial applications. Unscheduled downtime and maintenance activity on the compressors causes considerable loss in throughput and efficiency of a plant. Of all the failures that cause unscheduled downtime in reciprocating compressors, valve related causes are predominant. The objective of this paper is to research detection and prediction of valve failures by Multi-layer perceptron neural network, MLPANN, Radial basis function, RBFANN, and Group Method of Data Handling, GMDH analysis of pressure, temperature and vibration signals, which are the most common measurements on a reciprocating compressor system. These parameters are measured on a continuous basis and baselines are established for normal (or acceptable) behavior and failure (or fault) condition. In each model, the optimized structure is obtained through a Genetic algorithm, GA, technique. Quantitatively, the optimized MLPANN model achieved approximately 95% lower RMSE and 0.3% higher correlation coefficient compared with the RBFANN and GMDH models. Also, the MLPANN neural network demonstrated superior performance in fault diagnosis.

***Keywords*: Reciprocating compressors, Fault detection, Vlave, Machine learning.**

I. Introduction

Reciprocating compressors are among the most widely used types of positive displacement compressors, commonly employed across various industries. Their operation is based on the reciprocating motion of a piston within a cylinder. In the design of these compressors, the valve is considered a critical limiting component. These valves are often referred to as the "heart" of the compressor, as their failure can lead to complete compressor shutdown, resulting in significant disruptions and high costs. One of the most common issues encountered in these compressors is a reduction in output pressure or flow rate, typically caused by wear or failure of the valves. In fact, studies have shown that valves are responsible for up to 36% of unplanned shutdowns in reciprocating compressors [1-3]. This clearly demonstrates that valves are indeed the heart of these machines, and careful attention to their design is not merely desirable—it is essential. As a result, extensive research has been conducted on valve fault detection through experimental testing [4, 5], modeling techniques [6–8], and signal processing methods [9–12].

Compressor pressure can be effectively monitored using the pressure–volume (p–V) diagram, which is one of the most widely utilized process parameters in reciprocating compressors. Support Vector Machine (SVM) algorithms have been extensively applied in fault diagnosis based on p–V diagram analysis. Feng et al. [13] proposed a methodology for fault identification using p–V diagrams. Their approach combined Principal Component Analysis (PCA) for dimensionality reduction and a multiclass SVM classifier to detect five distinct types of valve faults in reciprocating compressors. Pichler et al. [14, 15] diagnosed valve faults in reciprocating compressors using features extracted from the p–V diagram. Specifically, the slope of the expansion phase, derived in logarithmic coordinates, and the difference between suction and discharge pressures were employed as features to train SVM classifiers. Their study focused on distinguishing between healthy and faulty conditions across six different valve types. Wang et al. [16] introduced an automated evaluation approach for the p–V diagram. They identified seven fixed points on the p–V curve and used these points as input features for classification using the SVM method. In a related study, Jiang et al. [17] conducted

* Manuscript received November 04, 2025, Revised November 29, 2025, Accepted February 03, 2026.

[1] Corresponding author. Assistant Professor, Mechanical Engineering Department, Sadjad University, Mashhad, Iran.
Email: hadi.kalani@gmail.com
[2] Atlas Petro Poyuseh Paj, Knowledge Based Company, Khorasan Science and Technology Park, Mashhad, Iran.
[3] Atlas Petro Poyuseh Paj, Knowledge Based Company, Khorasan Science and Technology Park, Mashhad, Iran.
[4] Associate Professor, Mechanical Engineering Department, Hakim Sabzevari University, Sabzevar, Iran.

research on fault identification in the p–V diagrams of reciprocating compressors using SVM. Fault-related features were extracted via a feature point extraction method, and a fault identification model was developed based on a multiclass SVM and a decision tree, using the derived feature vectors.

Artificial Neural Networks (ANNs) have also been employed in fault diagnosis based on p–V diagram analysis. Namdeo et al. [18] utilized ANN techniques to detect valve leakage in reciprocating compressors. The healthy expansion process of the compressor was predicted using a Functional Link Artificial Neural Network (FLANN). They applied the backpropagation algorithm to estimate the percentage of leakage based on deviations in pressure at a specific time point. In another study [19], features were extracted from raw pressure signals using wavelet packet decomposition. These features, combined with temperature data, were used to train a logistic regression model for valve fault classification.

Additionally, the extracted features were used to train a Recurrent Neural Network (RNN) in order to predict the future performance of the system. This predictive capability was shown to be useful for valve fault detection as well. Guo and et al. [20] used the ANN method for fault diagnosis of gas valves in reciprocating compressors based on the geometric features of the p–V diagram. The features were used to train a backpropagation (BP) neural network, which ultimately resulted in a 100% recognition rate. Guerra [21] extracted data from dynamic pressure signals using Fast Fourier Transform (FFT) and Principal Component Analysis (PCA) to detect valve failures through a Bayesian classifier at 50% and 100% loads. Besides the p–V diagrams, pressure measurements at other volumes can also be used for fault identification. Tiwari et al. [22] used an artificial neural network method for condition monitoring of a faulty reciprocating compressor. Corresponding values of pressure fluctuations in the outlet pipe were simulated to train the neural network for predicting the leakage percentage of the discharge valves. Guerra and Kolodziej [23] proposed a data-driven method for condition monitoring of reciprocating compressor valves. Fast Fourier Transform (FFT) was applied to the pressure wave measured around the discharge valve, and then the FFT values were divided into several frequency bands. After that, Principal Component Analysis (PCA) was used to reduce the dimensionality of the vectors. Finally, the results were used to train a Bayesian classifier, which was able to classify different levels of valve degradation with high accuracy.

Vibration analysis is another common method for condition monitoring of reciprocating compressors. Many faults in these compressors lead to abnormal vibrations, which can be detected through vibration signals containing rich information about the machine [24]. Qin and et.al [25] proposed a novel approach based on Support Vector Machine (SVM) that consisted of three stages: noise removal, feature extraction through wave matching, and classification using SVM. They achieved 100% accuracy.

Potocnik and et al. [10] developed a semi-supervised method based on vibration signals that included statistical evaluation and Principal Component Analysis (PCA) as a preprocessing step. Then, a comparative analysis was conducted between classification methods, including Discriminant Analysis (DA), Neural Networks (NN), Support Vector Machines (SVM), and Extreme Learning Machines (ELM). They demonstrated that nonlinear classifiers performed better. Pichler [26] proposed an independent method for valve fault detection based on vibration measurements using several different types of valves. Classifiers such as Logistic Regression (in the binary case) and SVM (in both binary and one-class cases) were compared. The results showed that all three classifiers performed equally well in detecting valve faults. Ahmed and et al. [27, 28] also conducted studies on fault classification in reciprocating compressors. They found that the classification performance of features extracted from the frequency domain was better than those extracted from the time domain when using a Probabilistic Neural Network (PNN). They also proposed a PNN optimized with a genetic algorithm, which achieved higher classification accuracy compared to the original version. Kolodziej and et al. [29] trained a Bayesian classifier for the early detection of spring fatigue and valve seat wear in reciprocating compressors and validated it with experimental data. Vibration data were processed using the Wigner–Ville spectrum and quantified with image-based statistical features. Then, Principal Component Analysis (PCA) was applied to reduce the feature space.

Although many studies have been conducted by researchers on the precise prediction of faults in reciprocating compressors, it remains challenging due to the importance and high cost of the equipment. In many investigations, vibration signals and other measured parameters (pressure and temperature) have been used separately to detect faults. However, this article employs a combination of these parameters. The main question addressed in this paper is which valve (intake or discharge, first or second stage) has developed a fault. To the best of the author's knowledge, there is no existing article that simultaneously uses a combination of vibration, pressure, and temperature parameters for fault diagnosis of reciprocating compressors. Filling this research gap can greatly assist the maintenance and repair unit of an industrial facility in preventing irreparable damage to these machines.

II. METHODOLOGY and DATA ACQUISITION

A. *Data Acquisition Equipment*

The experimental apparatus was designed to simulate multiple faults in a single-acting, two-stage reciprocating compressor. These simulated faults can be examined by comparing the healthy condition with the recorded data corresponding to each faulty condition, thereby facilitating machine condition analysis and fault diagnosis. In summary, this setup provides a flexible platform for compressor condition monitoring, allowing the implementation of various fault types within the system.

B. *A3P Reciprocating Compressor*

For experimental data acquisition, a reciprocating compressor manufactured by *Atlas Petro Pouyesh Paj* was utilized. The compressor housing consists of two piston–cylinder assemblies arranged at a 90-degree angle to each other, forming a “V” configuration. The experimental

reciprocating compressor is capable of compressing natural gas from an inlet pressure of 20 bar to an outlet pressure of approximately 60 bar. This is a two-stage, single-acting compressor. A heat exchanger is installed between the two cylinders to cool the hot compressed gas from the previous stage, thereby enhancing the compression ratio. The compressor is driven by a 90 kW electric motor, which transmits mechanical power to the crankshaft via a belt–pulley system connecting the motor and the compressor. The schematic diagram of the experimental setup is shown in Figure 1.



Fig. 1. The reciprocating compressor

C. Measurement Instruments

For data acquisition in this study, three pressure sensors, two temperature sensors, and one vibration sensor were utilized. These sensors were employed to collect data corresponding to various measurement parameters. All pressure, temperature, and vibration sensors were calibrated according to the manufacturer's specifications prior to data acquisition to ensure accurate and reliable measurements. Reciprocating compressors generally exhibit distinct frequency ranges that are closely associated with their operational characteristics and potential fault frequencies. In addition, an accelerometer model VTV122 was employed in this study. This accelerometer is of the velocity-type, designed to convert mechanical vibrations into corresponding electrical signals.

Fig. 2 illustrates a schematic representation of the accelerometer. The vibration sensor was mounted directly on the compressor casing to ensure accurate measurement of vibration responses.



Fig. 2. Vibration Sensor

The discharge pressure of cylinders in reciprocating compressors is of great importance. Therefore, the pressure sensor must be capable of measuring the entire desired pressure range. These sensors are also required to have a fast response time in order to accurately record rapid pressure variations. To monitor the discharge pressure of each cylinder, a WIKA IS-20-S pressure sensor was installed, as shown in Fig. 3.



Fig. 3. Pressure sensor

In a compressor, the gas temperature can rise exceptionally high during the compression cycle. To measure the temperature in each cylinder, thermocouples were employed with an operating range from 20 °C to 220 °C. As illustrated in Fig. 4, these thermocouples are of Type K and are used for monitoring the gas temperature at the cylinder outlets.



Fig. 4. Temperature sensor

The locations of the vibration, pressure, and temperature sensors are shown in Fig. 5.

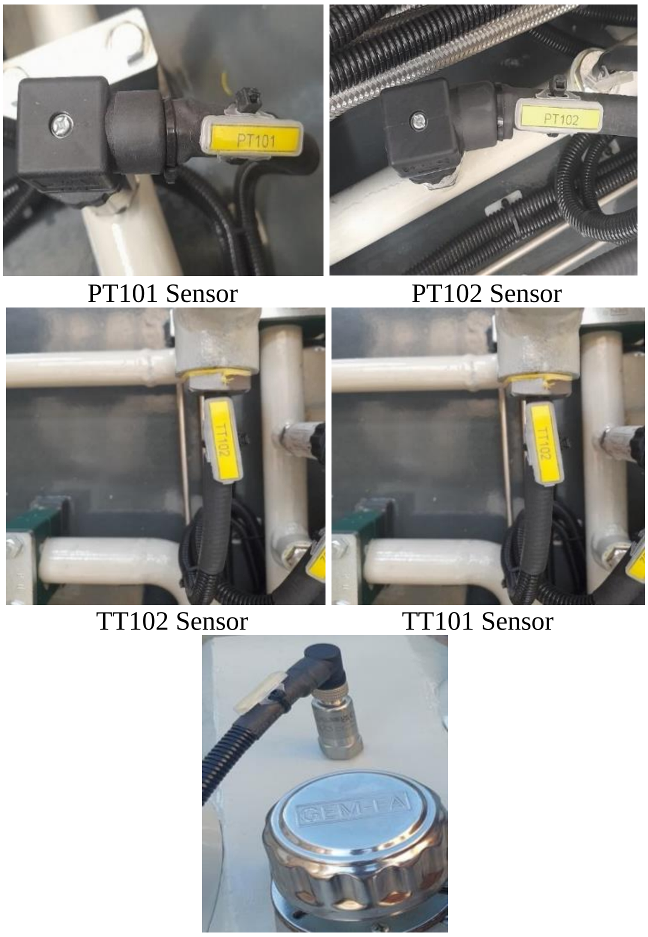


Fig. 5. Installation Locations of Sensors on the Reciprocating Compressor

As previously mentioned, in this study, three pressure sensors, two temperature sensors, and one vibration sensor were employed. According to Fig. 5, the sensors were installed as follows:

- PT100 sensor: Pressure sensor for measuring the gas pressure at the inlet of the first-stage cylinder.
- PT101 sensor: Pressure sensor for measuring the gas pressure at the outlet of the first-stage cylinder.
- PT102 sensor: Pressure sensor for measuring the gas pressure at the outlet of the second-stage cylinder.
- TT101 sensor: Temperature sensor for measuring the gas temperature at the outlet of the first-stage cylinder.
- TT102 sensor: Temperature sensor for measuring the gas temperature at the outlet of the second-stage cylinder.
- VT501 sensor: Vibration sensor for measuring the vibrations of the compressor block.

In this study, a Siemens S7-1200 PLC and a Siemens HMI were used, the specifications of which are shown in Fig. 6.

This PLC recorded the process variables with an effective sampling interval of approximately 1000 ms, using the PLC's native 16-bit integer and 32-bit floating-point formats. Logged data were stored on an external USB flash drive connected to the HMI via its built-in data logging function and exported in CSV format for offline analysis.



a) 6ES7 214-1AG40-0XB0



b) KTP700 Basic PN-6AV2123-2GB03-0AX0

Fig. 6. the view of PLC

D. *Valve fault*

To examine the effect of the introduced fault on the compressor's performance, an identical defect was created on the valve plates (Fig. 7). The defective disc was then installed separately on each inlet and outlet valve. Subsequently, the compressor was operated for half an hour, and data acquisition was performed. As previously mentioned, the pressure, temperature, and vibration parameters were recorded during this period.



Fig. 7. Fault on the Valve Disc

In this study, five classes were defined as follows:

- Class C1: All valves are in healthy condition.
- Class C2: The first-stage inlet valve is defective.
- Class C3: The first-stage outlet valve is defective.
- Class C4: The second-stage inlet valve is defective.
- Class C5: The second-stage outlet valve is defective.

E. *Machine Learning Methods*

1) Multilayer Perceptron Artificial Neural Network (MLPANN)

An MLPANN consists of a set of neurons arranged in multiple layers. Neurons in each layer can be connected to all or part of the neurons in adjacent layers through a series of weighted connections [30-33]. Therefore, the input to each neuron is a set of outputs from the previous layer's neurons, each multiplied by its corresponding weight. In general, each neuron can be considered as consisting of two separate parts.

In the first part, the sum of the inputs is computed, and in the second part, a function, referred to as the neuron activation function, is applied to this sum to calculate the neuron's output. Various functions can be used as the activation function, including the sign function, linear function, tangent sigmoid function, and logarithmic sigmoid function. Each of these functions has specific characteristics and can be applied in different scenarios. A general schematic of this network is shown in Fig. 8.

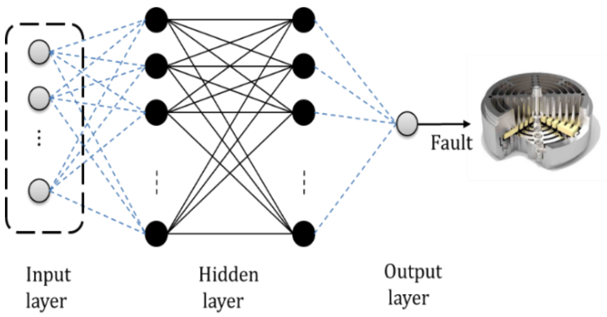


Fig. 8. Schematic of the MLPANN Neural Network Structure

2) Group Method of Data Handling (GMDH) Neural Network

Fig. 9 illustrates the architecture of this neural network. The GMDH algorithm is based on a set of neurons arranged in

multiple layers. In each layer, different pairs of neurons are connected using a second-degree polynomial [34]. In this way, they generate new neurons in the subsequent layer. Using this type of representation, the inputs can be mapped to the outputs. In this approach, a function $\hat{f}$, which can be considered as an approximation of the true function f, is employed so that for an input parameter vector $X = x_1, x_2, x_3, \dots x_n$, the output $\hat{y}_i$can be predicted as accurately as possible, ideally approaching the actual output. Consequently, for datasets with multiple inputs and a single output, the relationship can be expressed as:

$$y_i = f(x_{i1}, x_{i2}, x_{i3}, \dots, x_{in}) \; (i = 1,2, \dots, M) \quad (1)$$

Now, a GMDH-based neural network can be trained in such a way that it predicts the output values $\hat{y}_i$ for each input vector $X = x_{i1}, x_{i2}, x_{i3}, \dots, x_{in}$ following as

$$\hat{y} = \hat{f}\,(x_{i1}, x_{i2}, x_{i3}, \dots, x_{in})(i = 1,2, \dots, M) \quad (2)$$

The main challenge is to design a GMDH-type neural network in such a way that the squared differences between the actual and predicted outputs are minimized, that is,

$$\sum_{i=1}^{M} \left[\hat{f}\left(x_{i1,}x_{i2,}x_{i3}, \dots, x_{in}\right) - y_i\right]^2 \rightarrow min \quad (3)$$

The general relationships between the input and output parameters can be expressed using the discrete Volterra series form as follows:

$$y = a_0 + \sum_{i=1}^{n} a_i + \sum_{i=1}^{n} \sum_{j=1}^{n} a_{ij} x_i x_j + \sum_{i=1}^{n} \sum_{j=1}^{n} \sum_{k=1}^{n} a_{ijk} x_i x_j x_k + \cdots \quad (4)$$

where y is generally represented as a Kolmogorov-Gabor polynomial. The complete mathematical form can be expressed using a partial second-degree polynomial system that involves only two variables (neurons), as follows:

$$\hat{y} = G\left(x_i, x_j\right) = a_0 + a_1 x_i + a_2 x_j + a_3 x_i^2 + a_4 x_j^2 + a_5 x_i x_j \quad (5)$$

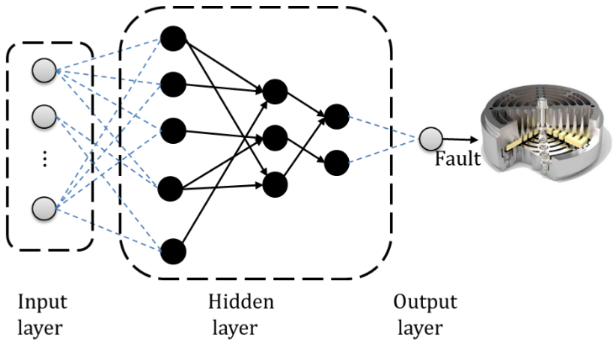


Fig. 9. Schematic of the GMDH Neural Network Structure

3) Radial Basis Function Neural Network (RBFNN)

Radial Basis Function Neural Networks (RBFNNs) are widely employed for non-parametric estimation of multidimensional functions using a limited set of training data. The basic architecture of an RBFNN consists of a two-layer network, as illustrated in Fig. 10. The hidden layer establishes a nonlinear mapping between the input space and a typically higher-dimensional space, playing a crucial role in transforming nonlinear patterns into linearly separable patterns [34, 35]. The output layer produces a weighted sum of the linearized patterns along with a linear output. When an RBFNN is used for function approximation, this output is sufficient. However, if pattern classification is required, a hard limiter or a sigmoid function can be applied to the output neurons to produce binary output values (0 or 1). The unique feature of this network lies in the processing performed within the hidden layer. The hidden layer function is defined as

$$F(x) = \sum_{j=1}^{p} w_j \phi(\|x - u_j\|) \quad (6)$$

where the w_j represent the weights associated with each neuron, and the u_j denote the centers of the neuron's activation function. A commonly used function in radial basis networks is the Gaussian or exponential function, expressed as

$$\phi(\|x - u_j\|) = e^{\frac{(\|x-u_j\|)}{\sigma_j}} \quad (7)$$

Where σ_j represents the kernel width factor of neuron.

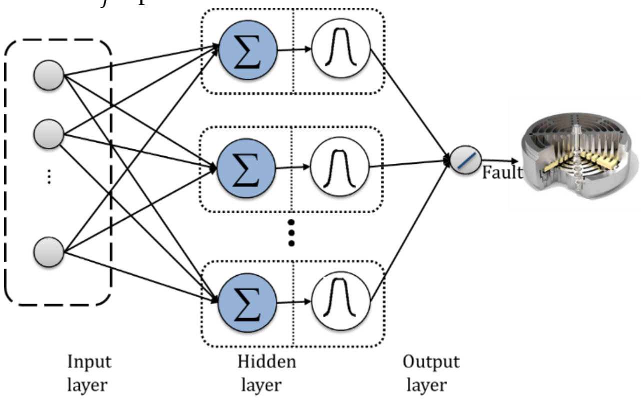


Fig. 10. Schematic of the RBF Neural Network Structure

F. Genetic Algorithm

The genetic algorithm (GA) was first proposed by Holland and later developed by other researchers. GA is part of evolutionary computation theory, which is currently experiencing rapid growth as a branch of artificial intelligence. The core idea of this algorithm is rooted in Darwin's theory of evolution. In this method, to optimize an objective function (fitness function) of a problem, an initial population of chromosomes (individuals), which essentially represent initial solutions to the problem, evolves into a new population representing secondary solutions. By iteratively generating new populations from the previous ones at each stage and producing successive generations, the population gradually converges toward an optimal solution [36-40]. In

this study, the genetic algorithm was used to determine suitable inputs and the optimal structure of the models for each individual. Fig. 11 illustrates the optimization process and the application of the genetic algorithm for model optimization. The Genetic Algorithm used for neural network optimization employed a population size of 50, with the evolutionary process executed for 100 generations. The convergence criterion was set such that the GA stopped when no improvement in the fitness value was observed over 20 consecutive generations.

III. Results

As previously mentioned, three pressure sensors, two temperature sensors, and one vibration sensor were employed. Fig. 12 presents a sample of the data acquired over approximately 30 minutes during the normal (healthy) operating condition of the compressor.

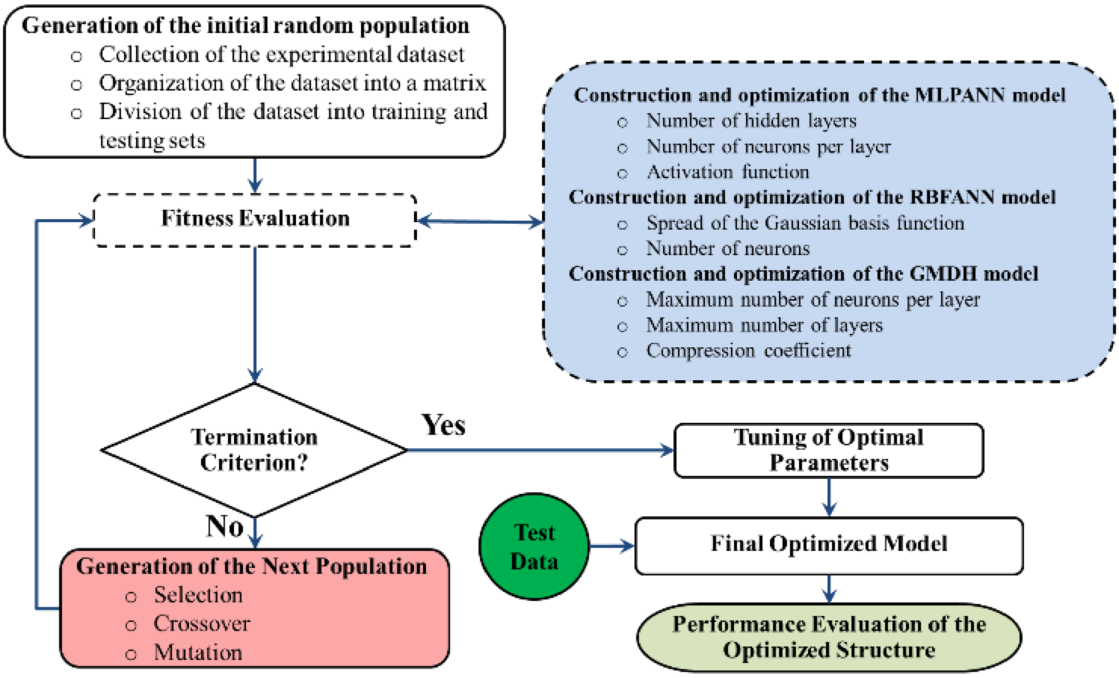
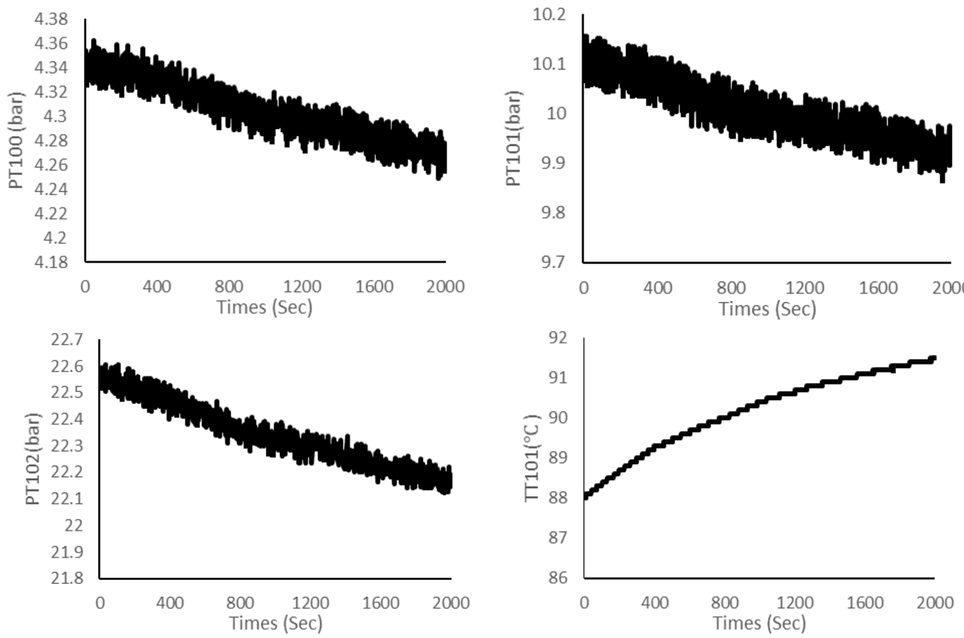


Fig. 11. Model Optimization Using the Genetic Algorithm



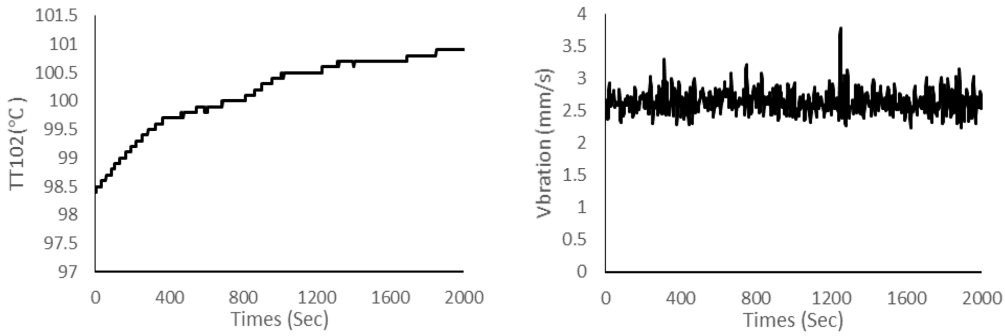


Fig. 12. Healthy operating data of the reciprocating compressor

For neural network simulation, MATLAB 2018 software was utilized. The present study was conducted on a system equipped with an Intel® Core i5-3570 CPU @ 3.40 GHz (up to 3.80 GHz), running a Windows operating system and a GTX 1080 graphics card. For modeling the neural networks, 70% of the data was used for training and the remaining 30% was allocated for validation and testing of the model. In this study, a 5-fold cross-validation procedure was applied to ensure the robustness and generalization capability of each model. Furthermore, to optimize the parameters of the neural networks using the Genetic Algorithm (GA), the optimization toolbox available in MATLAB was employed.

First, the objective function - the Mean Squared Error (MSE) of the neural network- was defined. Next, the parameters targeted for optimization were specified for the genetic algorithm. Finally, the best parameter values obtained through the optimization process were used for the final training of the neural networks. After applying the genetic algorithm to three neural network architectures - MLPANN, RBFANN and GMDH- the optimized key parameters for each model are summarized in Table 1.

Table 1-Optimized Parameters for Each Neural Network

Neural Network	Parameters and Optimization Range	Optimized Value
MLPANN	Activation function: [tansig, logsig]	logsig
	Number of neurons per layer: [5–30]	[15, 9]
	Number of hidden layers: [1–2]	2
RBFANN	Spread factor: [1–10]	9
	Maximum neurons: [5–30]	19
GMDH	Maximum neurons per layer: [5–30]	21
	Maximum number of layers: [2–40]	5
	Compression coefficient parameter: [0.2, 0.4, 0.6, 0.8]	0.4

As previously mentioned, in this study, three neural networks-MLPANN, RBFANN, and GMDH- optimized using the Genetic Algorithm (GA) were employed as classifiers. To evaluate the performance of these models, the following statistical indicators were used: Root Mean Square Error (RMSE), Correlation Coefficient (CC), and Average Absolute Error (AAE), which are defined as follows:

$$\mathrm{MSE} = 100 \times \frac{\sum_i (y_i - \hat{y}_i)^2}{\sum_i (y_i)^2} \tag{8}$$

$$\mathrm{CC} = 100 \times \frac{\sum_i (y_i \times \hat{y}_i)}{\sqrt{\sum_i (y_i)^2}\sqrt{\sum_i (\hat{y}_i)^2}} \tag{9}$$

$$\mathrm{AAE} = \frac{\sum_i |y_i - \hat{y}_i|}{n} \tag{10}$$

where n denotes the number of samples. Additionally y_i and $\hat{y}_i$ represent the actual (measured) output class and the predicted output class, respectively. In this study, the models were trained using 70% of the data, while the remaining 30% was reserved for testing the models.

Table 2- Values of RMSE (CC) [AAE] for the Three Neural Networks:MLPANN, RBFANN, and GMDH

	Healthy / Faulty	
	Train	Test
MLPANN	0.0 (100)[0.0]	0.034(99.98)[0.0016]
RBFANN	0.68(99.65)[0.024]	0.82(99.58)[0.0283]
GMDH	0.67(99.66)[0.0241]	0.628(99.68)[0.0235]

As shown in Table 2, the MLPANN neural network outperformed the other two methods in terms of prediction accuracy. To further compare the performance of the neural network models in fault prediction of the reciprocating compressor, an Analysis of Variance (ANOVA) was employed. In general, when the p-value is less than 0.05, it can be concluded that there is a significant difference between the performances of the two compared models. Table 3 presents the p-values obtained for fault prediction. As observed, in both cases, the p-value is greater than 0.05, indicating that there is no statistically significant difference among the three neural network models.

Table 3- p-values for Model Accuracy Comparison

		MLPANN	RBFANN	GMDH
P-Value	MLPANN	-	>0.05	>0.05

A confusion matrix is a performance evaluation tool used for assessing classification models in machine learning. It is represented as a two-dimensional table that displays the number of correct and incorrect predictions made by the model for each class. For a system with N classes, the confusion matrix is an N×N table. In binary classification problems, it consists of four key components: True Positives (TP), True Negatives (TN), False Positives (FP), and False Negatives (FN). As can be observed, only in the TN and TP cases are the predictions correct, while FP and FN represent misclassifications. To analyze this matrix, four important performance indicators are typically used: accuracy, true positive rate (sensitivity), precision (positive predictive value), and specificity. By comparing the averaged performance metrics across all data samples, Fig. 13 can be obtained. This figure illustrates which model demonstrates superior accuracy, stability, and statistical performance in data classification. The dataset considered in this study includes five classes (C1–C5).

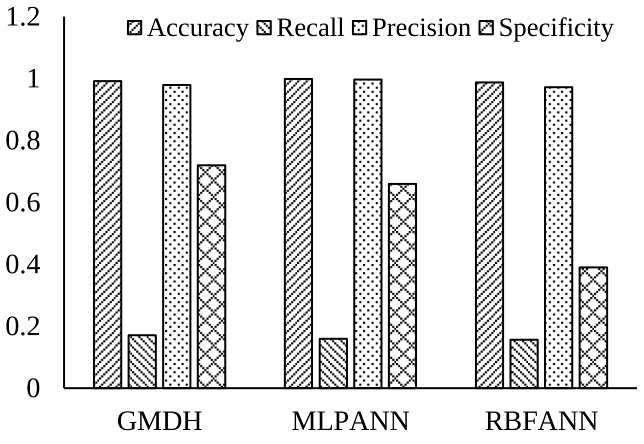


Fig. 13. Comparison of confusion matrix parameters

In terms of overall accuracy, the MLPANN model demonstrated the best performance across all classes, maintaining an almost constant value of 0.999. This indicates that MLPANN is highly reliable in terms of stability and consistency in data classification. In comparison, the GMDH model showed good performance but exhibited slight fluctuations across classes, while RBFANN performed worse than the other two models. Regarding the true positive rate (sensitivity), which reflects the model's ability to correctly identify positive samples, the GMDH model performed relatively better. This feature can be crucial in sensitive applications, such as disease detection or critical diagnostics, where missing a positive case could have serious consequences. However, an ANOVA test conducted on the true positive rates across different classes yielded a very high p-value (0.999), indicating no statistically significant difference among the three models in terms of positive predictive performance.

Overall, if the primary objective is stability, high accuracy, and consistent performance across all classes, the MLPANN model emerges as the superior choice. Based on the results, RBFANN demonstrates relatively lower performance on this dataset and is not a preferable option compared to the other two models. However, since the p-value is much greater than 0.05, there is no statistically significant difference among the three methods across the different classes. The overall performance of the models across classes C1 to C5 is illustrated in Fig. 14, which shows that all three models - GMDH, MLPANN, and RBFANN-perform relatively well in class C1, with minimal differences among them. This suggests that the data for C1 are likely simpler and more easily separable for the models.

Additionally, the figure indicates that RBFANN tends to perform worse in most classes and exhibits greater variability in results, making it less suitable for applications that require reliability and stability. In conclusion, the analysis highlights that MLPANN is the most appropriate option for achieving uniform and stable performance across all classes.

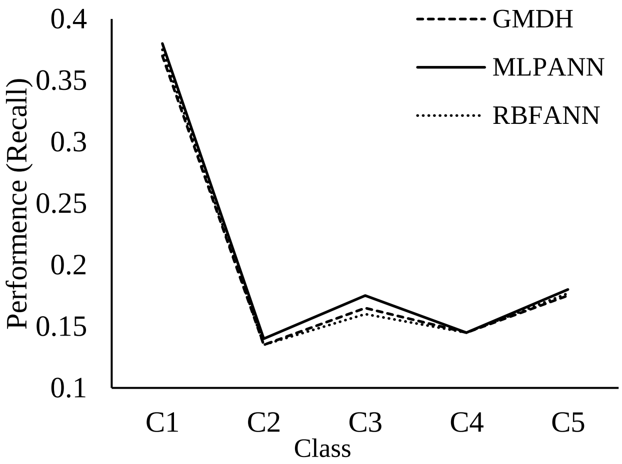


Fig. 14. Performance comparison of the three neural networks across different classes

IV. CONCLUSION

This study employed three different neural network models - MLPANN, RBFANN, and GMDH-for fault diagnosis of the inlet and outlet valves of reciprocating compressors. The primary objective was to accurately identify potential valve faults using compressor performance data and leveraging machine learning techniques. To enhance the accuracy and efficiency of the models, an optimization process using the Genetic Algorithm (GA) was applied to tune the parameters of each neural network. This algorithm automatically optimized parameters such as the number of neurons, learning rates, and network architecture, selecting the most suitable configuration to achieve the highest predictive accuracy. The use of GA improved the models' adaptability to the data and helped prevent overfitting.

Subsequently, the performance of all three models was evaluated and compared across multiple aspects, including accuracy, sensitivity, predictive precision, and specificity. Additionally, a statistical analysis, comprising Analysis of Variance (ANOVA), was conducted to assess the significance of differences among the model outcomes. The results indicated that the MLPANN model, with its very high accuracy and consistent performance across all fault classes, is the most suitable option for valve fault detection. Meanwhile, GMDH demonstrated relative superiority in certain classes, particularly in terms of sensitivity.

Ultimately, by integrating both numerical and statistical analyses, MLPANN was identified as the optimal and superior neural network model. This model not only exhibited high fault detection accuracy but also maintained stable performance across all fault classes and demonstrated practical applicability for real-world operational conditions.

REFERENCES

[1] N. Dobrivoje et al., "Modelling Valve Dynamics and Flow in Reciprocating Compressors," 2013.

[2] Z. Zhang et al., "Fault Diagnosis of Reciprocating Compressor Valve Based on Triplet Siamese Neural Network," *Machines*, vol. 13, no. 4, p. 263, 2025. https://doi.org/10.3390/machines13040263

[3] R. Medina et al., "Scale-fractal detrended fluctuation analysis for fault diagnosis of a centrifugal pump and a reciprocating compressor," *Sensors*, vol. 24, no. 2, 2024. https://doi.org/10.3390/s24020461

[4] F. Bie et al., "Research on fault diagnosis method of reciprocating compressor valve based on IVMD-CMS model," *Journal of Mechanical Science and Technology*, vol. 37, no. 8, pp. 3931-3943, 2023. https://doi.org/10.1007/s12206-023-0709-x

[5] W. Wu et al., "A new method for reciprocating compressor fault diagnosis based on indicator diagram feature extraction," *Proceedings of the Institution of Mechanical Engineers, Part A: Journal of Power and Energy*, vol. 237, no. 6, pp. 1337-1347, 2023. https://doi.org/10.1177/09576509231161855

[6] M. A. Elhaj, *Condition monitoring of reciprocating compressor valves*. The University of Manchester (United Kingdom), 2005.

[7] F. Liu et al., "An experimental study on engine dynamics model based in-cylinder pressure estimation," SAE Technical Paper, 0148-7191, 2012. https://doi.org/10.4271/2012-01-0896

[8] F. V. Tinaut et al., "Misfire and compression fault detection through the energy model," *Mechanical Systems and Signal Processing*, vol. 21, no. 3, pp. 1521-1535, 2007. https://doi.org/10.1177/0954407020987077

[9] M. Ahmed et al., "Fault detection and diagnosis using Principal Component Analysis of vibration data from a reciprocating compressor," in *Proceedings of 2012 UKACC International Conference on Control*, 2012: IEEE, pp. 461-466. https://doi.org/10.1109/CONTROL.2012.6334674

[10] P. Potočnik and E. Govekar, "Semi-supervised vibration-based classification and condition monitoring of compressors," *Mechanical Systems and Signal Processing*, vol. 93, pp. 51-65, 2017. https://doi.org/10.1016/j.ymssp.2017.01.048

[11] C. Ruiz-Cárcel, V. H. Jaramillo, D. Mba, J. R. Ottewill, and Y. Cao, "Combination of process and vibration data for improved condition monitoring of industrial systems working under variable operating conditions," *Mechanical Systems and Signal Processing*, vol. 66, pp. 699-714, 2016. https://doi.org/10.1016/j.ymssp.2015.05.018

[12] Z. Sun et al., "Instability detection of centrifugal compressors by means of acoustic measurements," *Aerospace Science and Technology*, vol. 82, pp. 628-635, 2018. https://doi.org/10.1016/j.ast.2018.09.006

[13] K. Feng et al., "A recognition and novelty detection approach based on Curvelet transform, nonlinear PCA and SVM with application to indicator diagram diagnosis," *Expert Systems with Applications*, vol. 38, no. 10, pp. 12721-12729, 2011. https://doi.org/10.1016/j.eswa.2011.04.060

[14] K. Pichler et al., "Detecting broken reciprocating compressor valves in the pV diagram," in *2013 IEEE/ASME International Conference on Advanced Intelligent Mechatronics*, 2013, pp. 1625-1630. https://doi.org/10.1109/AIM.2013.6584329

[15] K. Pichler et al., "Detecting cracks in reciprocating compressor valves using pattern recognition in the pV diagram," *Pattern Analysis and Applications*, vol. 18, pp. 461-472, 2015. https://doi.org/10.1007/s10044-014-0431-5

[16] F. Wang, L. Song, L. Zhang, and H. Li, "Fault diagnosis for reciprocating air compressor valve using pV indicator diagram and SVM," in *2010 Third International Symposium on Information Science and Engineering*, 2010: IEEE, pp. 255-258. https://doi.org/10.1109/ISISE.2010.91

[17] Z. Jiang et al., "Research on reciprocating compressor indicator diagram fault recognition based on support vector machine," *Fluid Machinery*, vol. 40, pp. 21-25, 2012.

[18] R. Namdeo et al., "Detection of valve leakage in reciprocating compressor using artificial neural network (ANN)," 2008.

[19] M. C. Leu et al., "Computer program and method for detecting and predicting valve failure in a reciprocating compressor," ed: Google Patents, 2010.

[20] F.-Y. Guo et al., "Fault diagnosis of reciprocating compressor valve based on transfer learning convolutional neural network," *Mathematical Problems in Engineering*, vol. 2021, no. 1, p. 8891424, 2021. https://doi.org/10.1155/2021/8891424

[21] C. J. Guerra, *Condition monitoring of reciprocating compressor valves using analytical and data-driven methodologies*. Rochester Institute of Technology, 2013.

[22] P. Kumar and R. Tiwari, "A review: multiplicative faults and model-based condition monitoring strategies for fault diagnosis in rotary machines," *Journal of the Brazilian Society of Mechanical Sciences and Engineering*, vol. 45, no. 5, p. 282, 2023. https://doi.org/10.1007/s40430-023-04203-z

[23] C. J. Guerra and J. R. Kolodziej, "A data-driven approach for condition monitoring of reciprocating compressor valves," *Journal of Engineering for Gas Turbines and Power*, vol. 136, no. 4, p. 041601, 2014. https://doi.org/10.1115/1.4025944

[24] M. Karimi and S. Aliabadi, "Automated Fault Detection of Tri-Lobe Compressor Using Wavelet Transformation and Support Vector Machine," *Journal Of Applied and Computational Sciences in Mechanics*, vol. 27, no. 1, pp. 19-34, 2016.

[25] Q. Qin et al., "A novel scheme for fault detection of reciprocating compressor valves based on basis pursuit, wave matching and support vector machine," *Measurement*, vol. 45, no. 5, pp. 897-908, 2012. https://doi.org/10.1016/j.measurement.2012.02.005

[26] K. Pichler, "Early Fault Detection in Reciprocating Compressor Valves by Means of Vibration and pV Diagram Analysis," in *Predictive Maintenance in Dynamic Systems: Advanced Methods, Decision Support Tools and Real-World Applications*: Springer, 2019, pp. 167-205. https://doi.org/10.1007/978-3-030-05645-2_6

[27] M. Ahmed, S. Abdusslam, M. Baqqar, F. Gu, and A. D. Ball, "Fault classification of reciprocating compressor based on neural networks and support vector machines," in *The 17th International Conference on Automation and Computing*, 2011: IEEE, pp. 213-218.

[28] M. Ahmed et al., "Feature selection and fault classification of reciprocating compressors using a genetic algorithm and a probabilistic neural network," in *Journal of Physics: Conference Series*, 2011, vol. 305, no. 1: IOP Publishing, p. 012112. https://doi.org/10.1088/1742-6596/305/1/012112

[29] J. R. Kolodziej and J. N. Trout, "An image-based pattern recognition approach to condition monitoring of reciprocating compressor valves," *Journal of Vibration and Control*, vol. 24, no. 19, pp. 4433-4448, 2018. https://doi.org/10.1177/1077546317726453

[30] H. Kalani et al., "Using artificial neural network models and particle swarm optimization for manner prediction of a photovoltaic thermal nanofluid based collector," *Applied Thermal Engineering*, vol. 113, pp. 1170-1177, 2017. https://doi.org/10.1016/j.applthermaleng.2016.11.105

[31] H. Kalani et al., "Forward kinematics solution of stewart-gough using improved hybrid strategy (neural network and 3rd-order Newton-Raphson," *Journal of Computational Methods in Engineering*, vol. 35, no. 2, pp. 113-129, 2022. https://doi.org/10.18869/acadpub.jcme.35.2.113

[32] A. Sadollah and J. Riazat, "Parameter Optimization of Various Solar Cell Models by Neural Network Algorithm," *Journal Of Applied and Computational Sciences in Mechanics*, vol. 36, no. 1, pp. 123-142, 2024. https://doi.org/10.22067/jacsm.2023.81702.1176

[33] M. Zamani mohiabadi et al., "Flow prediction in two-dimensional asymmetric diffuser by neural network and comparison with three turbulence models and experimental data," *Journal Of Applied and Computational Sciences in Mechanics*, vol. 34, no. 2, pp. 45-60, 2022. https://doi.org/10.22067/jacsm.2022.74041.1076

[34] H. J. Salmani et al., "Predicting the performance of organic solvent reverse osmosis membranes using artificial neural network and principal component analysis by considering solvent–solvent and solvent–membrane affinities," *Journal of Membrane Science*, vol. 687, p. 122025, 2023. https://doi.org/10.1016/j.memsci.2023.122025

[35] H. Jalaei Salmani et al., "A practical hybrid machine learning method for predicting the flash point of complex ternary alcohol-based mixtures," *Petroleum Science and Technology*, vol. 42, no. 25, pp. 4390-4404, 2024. https://doi.org/10.1080/10916466.2023.2246489

[36] H. Kalani et al., "Multi-objective genetic algorithm and Castigliano’s theorem for stiffness optimisation of parallel robots: case study of conventional Stewart platforms," *Australian Journal of Mechanical Engineering*, vol. 22, no. 4, pp. 797-809, 2024. https://doi.org/10.1080/14484846.2023.2174281

[37] H. Kalani and A. Akbarzadeh, "Multiple-objective Optimization of Serpentine Locomotion with Snake Robot by Using the NSGA," 2012.

[38] M. Beynaghi et al., "Analysis of fracture behavior of carbon nitride poly crystalline by genetic algorithm and molecular dynamics methods," *Journal Of Applied and Computational Sciences in Mechanics*, vol. 36, no. 2, pp. 29-46, 2024. https://doi.org/10.22067/jacsm.2023.83323.1192

[39] M. sargolzaie, A. tousi, and r. askari, "Optimization of one Stage Axial Compressor by using Quasi-Three Dimensional Design and Hybrid Genetic Algorithm," *Journal Of Applied and Computational Sciences in Mechanics*, vol. 26, no. 1, pp. 63-78, 2015.

[40] M. Delkhosh and M. Saadat Foumani, "Geometric Optimization of Half Toroidal Continuously Variable Transmission Using Intelligent Techniques," *Journal Of Applied and Computational Sciences in Mechanics*, vol. 23, no. 1, pp. 29-40, 2012. https://doi.org/10.22067/FUM-MECH.V23I1.12819